## Polarization hydrodynamics in a one-dimensional polariton condensate

P.-É. Larré,<sup>1</sup> N. Pavloff,<sup>1</sup> and A. M. Kamchatnov<sup>2</sup>

<sup>1</sup>Univ. Paris Sud, CNRS, Laboratoire de Physique Théorique et Modèles Statistiques, UMR8626, F-91405 Orsay, France

<sup>2</sup>Institute of Spectroscopy, Russian Academy of Sciences, Troitsk, Moscow, 142190, Russia

We study the hydrodynamics of a nonresonantly-pumped polariton condensate in a quasi-onedimensional quantum wire taking into account the spin degree of freedom. We clarify the relevance of the Landau criterion for superfluidity in this dissipative two-component system. Two Cherenkovlike critical velocities are identified corresponding to the opening of different channels of radiation: one of (damped) density fluctuations and another of (weakly damped) polarization fluctuations. We determine the drag force exerted onto an external obstacle and propose experimentally measurable consequences of the specific features of the fluctuations of polarization.

PACS numbers: 47.37.+q,03.75.Mn,71.36.+c

The condensation of exciton-polaritons in semiconductor microcavity<sup>1-4</sup> arouse a great interest directed towards the possible demonstration of superfluid dynamics in coupled light-matter waves. Beautiful experiments revealed suppression of back-scattering from an obstacle<sup>5,6</sup>. nucleation of quantized vortices<sup>7-10</sup>, and generation of effectively stable oblique solitons<sup>11,12</sup> (see also the review article 13 and references therein). Although the definition of a genuine superfluid behavior in these systems is still a matter of active debates (see, e.g., the exchange in Refs. 14), it makes no doubt that the coherent wavemechanical flow of an exciton-polariton condensate offers the prospect of studying a rich variety of remarkable hydrodynamic effects. Among these, the specific features associated to the spin of the exciton-polaritons are of particular interest. In the hydrodynamic context they have been revealed by the observation of the optical spin Hall effect<sup>15</sup>, of half vortices<sup>16</sup>, and of half solitons<sup>17</sup>.

In the present work we concentrate on linear spin effects: nonlinear effects are addressed in an other publication<sup>18</sup>. We describe the polariton condensate by a two-component order parameter  $\psi_{\pm}$  accounting for the spin degree of freedom, corresponding to the two possible excitonic spin projections  $\pm 1$  onto the structure growth axis and to the right and left circular polarization of emitted photons. Interactions within the system can be described by two constants  $\alpha_1$  and  $\alpha_2$  corresponding to interactions between polaritons with parallel  $(\alpha_1)$  or antiparallel ( $\alpha_2$ ) spins. It is accepted that  $\alpha_1 > 0$  and that  $|\alpha_2| < \alpha_1$  [see the discussion after Eqs. (2)]. In the following we always consider the standard situation where  $0 < -\alpha_2 < \alpha_1$ . In the presence of an external magnetic field applied parallel to the structure axis, there is a Zeeman splitting  $2\hbar\Omega$  between the two circularly polarized states  $\psi_+$  and  $\psi_-$  (we neglect the possible small residual splitting of linear polarization considered for instance in Ref. 19). Taking into account the effect of the external magnetic field and of the interactions amongst polaritons, one can write the energy density of the uniform system  $as^{20}$ 

$$E = -\hbar \Omega \left(\rho_{+}^{0} - \rho_{-}^{0}\right) + \frac{\alpha_{1}}{2} \left[ (\rho_{+}^{0})^{2} + (\rho_{-}^{0})^{2} \right] + \alpha_{2} \rho_{+}^{0} \rho_{-}^{0}, \quad (1)$$

where  $\rho_{\pm}^{0} = |\psi_{\pm}^{0}|^{2}$  is the (uniform) density of polaritons with spin ±1, and in the following we denote the total density of the polariton gas as  $\rho^{0} = \rho_{+}^{0} + \rho_{-}^{0}$ . Then, minimizing the free energy of the system, one finds two regimes<sup>20</sup>. For large magnetic field  $[\hbar \Omega > \hbar \Omega_{\rm crit} = \frac{1}{2}(\alpha_{1} - \alpha_{2})\rho^{0}]$  the system is circularly polarized with  $\rho_{-}^{0} = 0$ , and the chemical potential reads  $\mu = \alpha_{1}\rho^{0} - \hbar \Omega$ . For lower fields  $(\hbar \Omega < \hbar \Omega_{\rm crit})$  the polarization gradually becomes linear when  $\Omega$  decreases; in this case one has

$$\rho_{\pm}^{0} = \frac{1}{2}\rho^{0} \left(1 \pm \Omega/\Omega_{\text{crit}}\right) \quad \text{and} \quad \mu = \frac{1}{2}(\alpha_{1} + \alpha_{2})\rho^{0}, \quad (2)$$

from which it is clear that, in the absence of magnetic field (that is, when  $\Omega = 0$ ), the system is linearly polarized<sup>1,2</sup>, a feature that originates in the present phenomenological description from the positiveness of  $\alpha_1 - \alpha_2$ . The fact that  $\alpha_1 + \alpha_2 > 0$  implies that  $\mu > 0$ , that the uniform polariton gas is stable, and that it corresponds to an emission blue shift<sup>1,21,22</sup>.

A study of spin dynamics has been done in Ref. 23 in the case of a fully polarized ground state. In the present work we treat instead the weak magnetic field regime (2), and study the dynamics of the system in the presence of (i) an external potential representing an obstacle and/or of (ii) modulations of the uniform ground state. We consider a one-dimensional wire-shaped cavity structure in which the order parameter is of the form  $\psi_{\pm}(x,t)$  and we model the dynamics of the system by the following Gross-Pitaevskii-type equation:

$$i\hbar \partial_t \psi_{\pm} = -\frac{\hbar^2}{2m} \partial_x^2 \psi_{\pm} + U_{\text{ext}}(x+Vt) \psi_{\pm} \mp \hbar \Omega \psi_{\pm} + (\alpha_1 \rho_{\pm} + \alpha_2 \rho_{\mp}) \psi_{\pm} + i (\gamma - \Gamma \rho) \psi_{\pm}, \quad (3)$$

where *m* is the polariton effective mass (in the parabolic dispersion approximation, valid at small momenta) and  $\rho_{\pm}(x,t) = |\psi_{\pm}(x,t)|^2$ .  $U_{\text{ext}}(x+Vt)$  describes an obstacle in motion at velocity *V* with respect to the polariton fluid. In accordance with the description (1), the effect of the magnetic field is accounted for in Eq. (3) by the Zeeman term  $\mp \hbar \Omega \psi_{\pm}$  and interaction effects are described by local terms proportional to  $\alpha_1$  and  $\alpha_2$ . Due to the finite polariton-lifetime, the system needs to be pumped.

Following Refs. 24–27 we schematically describe this effect by the last term of Eq. (3): The term  $i \gamma \psi_{\pm}$  describes the combined effects of the incoherent pumping and decay processes;  $\gamma > 0$ , indicating an overall gain counterbalanced by the term  $-i\Gamma\rho \psi_{\pm}$  (where  $\Gamma > 0$  and  $\rho = \rho_+ + \rho_-$ , which phenomenologically accounts for a saturation of the gain at large density and makes it possible to reach a steady-state configuration with a finite density  $\rho^0 = \gamma/\Gamma$ . Note that the saturation term is proportional to  $\rho$ . Arguing on weak cross-spin scattering, the authors of Ref. 28 used a different type of saturation of the gain, proportional to  $\rho_{\pm}$ : In this case the value of the stationary background densities  $\rho^0_+$  and  $\rho^0_-$  is fixed a priori, independently of the magnetic field. In the present work we follow Ref. 29 and use a model where the value of  $\rho^0_+$  and  $\rho^0_-$  is fixed by the thermodynamic equilibrium between the two spin components in the presence of a magnetic field [Eqs. (2)].

A small departure from the stationary configuration (2) is described by an order parameter of the form

$$\psi_{\pm}(x,t) = \psi_{\pm}^{0} \left[ 1 + \varphi_{\pm}(x,t) \right] \exp(-i\,\mu \,t/\hbar), \qquad (4)$$

where  $|\varphi_{\pm}(x,t)| \ll 1$ . In the absence of external potential  $(U_{\text{ext}} = 0)$ , the  $\varphi_{\pm}(x,t)$ 's which are solutions of the linearized version of Eq. (3) are plane waves whose wavevector q and frequency  $\omega$  are related by

$$0 = \omega^{4} + 2i\gamma\omega^{3} - \left(\frac{q^{4}}{2} + \frac{2}{1+\alpha}q^{2}\right)\omega^{2}$$
$$- 2i\gamma\left(\frac{q^{4}}{4} + 4\varrho_{+}^{0}\varrho_{-}^{0}\frac{1-\alpha}{1+\alpha}q^{2}\right)\omega$$
$$+ \frac{q^{4}}{4}\left(\frac{q^{4}}{4} + \frac{2}{1+\alpha}q^{2} + 16\varrho_{+}^{0}\varrho_{-}^{0}\frac{1-\alpha}{1+\alpha}\right).$$
(5)

In this equation we note  $\alpha = \alpha_2/\alpha_1$  (-1 <  $\alpha$  < 0),  $\varrho_{\pm}^0 = \rho_{\pm}^0/\rho^0 = \frac{1}{2}(1 \pm \Omega/\Omega_{\rm crit})$ , and we use dimensionless quantities: Energies are henceforth expressed in units of  $\mu$ , lengths in units of  $\xi$  [where  $\xi = \hbar/(m \mu)^{1/2}$ ], and velocities in units of  $(\mu/m)^{1/2}$ . Equation (5) has already been obtained in Ref. 30 in the case of a two-component Bose gas (i.e., in the absence of damping:  $\gamma = 0$ ) without magnetic field.

Solving the fourth-degree equation (5) yields the dispersion relations  $\omega = \omega(q)$ . If  $\omega(q)$  is a solution, then  $-\omega^*(q)$  is also a solution. As a result, the solutions come into pairs having either the same zero real part or the same imaginary part and opposite real parts. Some typical dispersion relations are plotted in Fig. 1. In the limit of weak magnetic field one pair of solutions corresponds to the usual density-fluctuation mode (in which both components oscillate in phase), the other one to a polarization-fluctuation mode (with counterphase oscillations of the two components). We henceforth keep using the denominations "density mode" and "polarization mode" although the separation between the two types of fluctuations is less strict for finite magnetic field, as illustrated in the lower row of Fig. 1 where we plot the contribution of each mode to the static structure factor  $S(q) = \int S(q, \omega) d\omega$ , where  $S(q, \omega)$  is the (zero temperature) dynamical structure factor<sup>31</sup>. The fact that one of the contributions can be negative originates in the non conservative nature of Eq. (3), but it is interesting to note that, despite its losses, the system keeps a constant density and still verifies the *f*-sum rule:  $\int_0^\infty \omega S(q, \omega) d\omega = \rho_0 q^2/2.$ 

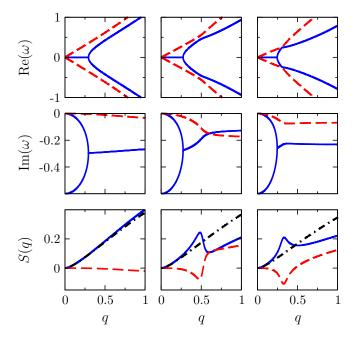


Figure 1. (Color online) Dispersion relations in the case  $\alpha = -0.2$  and  $\gamma = 0.3^{32}$ . The first (second) row displays  $\operatorname{Re}(\omega)$  [Im( $\omega$ )] as a function of q. The lower row displays the contribution of the density and polarization modes to the total density structure factor S(q) (black dot-dashed line). In each plot the blue solid curve corresponds to the density mode and the red dashed curve to the polarization mode. The three columns are drawn in the cases (from left to right)  $\Omega/\Omega_{\rm crit} = 0.2, 0.5, \text{ and } 0.7.$ 

From Eq. (5) one can show that the polarization mode is undamped (i) when  $\varrho_+^0 = \varrho_-^0 = \frac{1}{2}$ , i.e., in the absence of magnetic field, and (ii) when  $\varrho_{-}^{0} = 0$ , i.e., at the critical magnetic field. This is a first hint indicating that the damping of the polarization mode is weak. One can further show that this damping is zero up to order  $O(\Omega^2)$ in the external magnetic field. A final evidence comes from the fact that the damping of the polarization mode is always zero in the long-wavelength limit as we discuss now. In the absence of damping and of magnetic field  $(\gamma = 0 \text{ and } \Omega = 0, \text{ respectively})$  the long-wavelength behavior of both modes corresponds to a linear dispersion relation: The system exhibits two types of sound. One is the usual sound of velocity  $c_{\rm d} = 1$ . The other is the "polarization sound" of velocity  $c_{\rm p} = [(1-\alpha)/(1+\alpha)]^{1/2}$ . For nonzero  $\gamma$  the usual sound waves are damped; this is not the case for the polarization sound, as clearly seen in Fig. 1. In the general case where  $\gamma$  and  $\Omega$  are

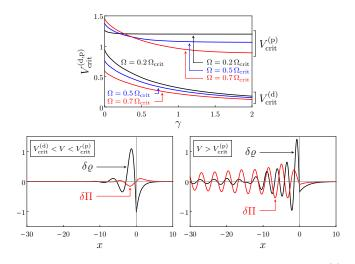


Figure 2. (Color online) Upper panel: Critical velocities  $V_{\rm crit}^{\rm (d)}$ and  $V_{\rm crit}^{\rm (p)}$  as a function of  $\gamma$  for different strengths of the magnetic field. The plot is drawn when  $\alpha = -0.2$ . Lower panels: Rescaled fluctuations of the density  $[\delta \varrho(x)/\varkappa$ : black curves] and of the polarization  $[\delta \Pi(x)/\varkappa$ : red curves] induced by a  $\delta$ -peak potential  $\varkappa \delta(x + Vt)$ . The modulation patterns are drawn for  $\alpha = -0.2$ ,  $\gamma = 0.2$ , and  $\Omega/\Omega_{\rm crit} = 0.1$ . In this case,  $V_{\rm crit}^{\rm (d)} = 0.69(4)$  and  $V_{\rm crit}^{\rm (p)} = 1.21(9)$ . The figures are drawn in the frame where the obstacle stays at rest at the origin and where the polariton fluid moves from left to right at velocity V > 0. For the lower left panel V = 1.1 and for the lower right panel V = 1.5.

nonzero, looking for a solution of Eq. (5) under the form  $\omega(q) = c_{\rm p} q$ , in the limit  $|q| \ll 1$  and  $c_{\rm p}|q| \ll \gamma$  one gets  $c_{\rm p} = [(1 - \Omega^2/\Omega_{\rm crit}^2)(1 - \alpha)/(1 + \alpha)]^{1/2}$ .

From the knowledge of the dispersion relations one can compute the linear response function  $\chi_{\pm}(q,\omega)$ which characterizes how the rescaled density  $\rho_{\pm}(x,t) =$  $\rho_{\pm}(x,t)/\rho^0$  responds to a weak external scalar potential with wavevector q and pulsation  $\omega$ . This makes it possible to determine the wake generated by a weakly perturbing obstacle moving at constant velocity V with respect to the polariton fluid. We do not detail the computation which has been presented in Ref. 33 in the case of a scalar order parameter. In the present case, there exist two particular velocities corresponding to the opening of channels of (damped) Cherenkov radiation:  $V_{\text{crit}}^{(d)}$  is the threshold for emission of density waves and  $V_{\text{crit}}^{(p)}$  is the threshold for emission of polarization waves. These velocities are functions of the losses in the system (i.e., of  $\gamma$ ) and of the strength of the external magnetic field (i.e., of  $\Omega$ ). They are represented in Fig. 2.

The physical meaning of these velocities can be verified by inspecting the perturbations induced by the obstacle which are represented in Fig. 2 in the simplest case where the external potential is of the form  $U_{\text{ext}} = \varkappa \, \delta(x + Vt)$ . The plots are drawn in the frame where the obstacle is at rest at the origin and where the polariton fluid moves from left to right at velocity V > 0. In this frame the perturbations are stationary. In Fig. 2 we do not display separately  $\delta \varrho_+ = \varrho_+ - \varrho_+^0$  and  $\delta \varrho_- = \varrho_- - \varrho_-^0$  but we rather plot the relevant physical observables: the fluctuations of the total density ( $\delta \varrho = \delta \varrho_+ + \delta \varrho_-$ ) and of the polarization ( $\delta \Pi = \delta \varrho_+ - \delta \varrho_-$ ). The critical velocity  $V_{\rm crit}^{\rm (p)}$ being larger than  $V_{\rm crit}^{\rm (d)}$ , an obstacle whose velocity V relative to the condensate lies between these two critical velocities (such as considered in the lower left plot of Fig. 2) only emits density fluctuations<sup>34</sup>. On the contrary, when V is larger than both  $V_{\rm crit}^{\rm (d)}$  and  $V_{\rm crit}^{\rm (p)}$ , the wake consists in both density and polarization fluctuations (see Fig. 2, lower right plot). We also note that a direct computation of the density patterns  $\varrho_{\pm}$  for several intensities of the magnetic field shows that, as stated above, the polarization wave is weakly damped at low and at high field, facilitating the experimental observation of the polarization signal compared to that of density fluctuations.

The existence of two critical velocities has also an important effect on the behavior of the drag force  $F_d$  experienced by the obstacle. This is illustrated in Fig. 3 where  $F_d$  is plotted as a function of V for two types of obstacles: a point-like scatterer of intensity  $\varkappa$ , for which  $U_{\text{ext}} =$  $\varkappa\,\delta(x+Vt),$  and a Gaussian potential of same intensity and of width  $\ell$ , for which  $U_{\text{ext}} = \frac{\varkappa}{\ell\sqrt{\pi}} \exp[-(x+Vt)^2/\ell^2]$ . One sees in Fig. 3 that, at very weak damping,  $F_d$  is negligible at small velocity and shows pronounced thresholds when V reaches the critical velocities  $V_{\text{crit}}^{(d)}$  and  $V_{\text{crit}}^{(p)}$ , demonstrating that in the limit  $\gamma \to 0$  the drag uniquely consists in wave resistance. This corresponds to the Landau criterion for the onset of dissipation: At each opening of a radiation channel (i.e., at  $V = V_{\text{crit}}^{(d)}$  and  $V_{\text{crit}}^{(p)}$ ) the drag is abruptly increased. This reflects the work imparted to the fluid and dissipated by generating the wave pattern which irreversibly radiates energy away from the obstacle. For finite values of  $\gamma$  instead, the flow is never truly superfluid: The obstacle experiences a finite force even at low velocity $^{27,35}$ , which corresponds to diffusion of momentum, i.e., to a viscous drag. In this case there is no Landau criterion, but the system exhibits a smooth crossover from a drag dominated by viscous-like phenomena (at low velocity) to one dominated by wave resistance (at large velocity). Thus, it is more appropriate to term the velocities  $V_{\rm crit}^{(d)}$  and  $V_{\rm crit}^{(p)}$  Cherenkov- (or Mach-) rather than Landau-critical velocities.

We also note that in the absence of external magnetic field (in the case  $\Omega = 0$ , not shown in the figure) no step is seen in the drag, even for  $\gamma \to 0$ . This is due to the fact that, despite the opening of a new radiation channel at  $V = V_{\rm crit}^{\rm (d)}$ , the external scalar potential cannot excite polarization waves in this case for symmetry reasons, since no term in Eq. (3) can distinguish the spin-up from the spin-down component when  $\Omega = 0$ . This is reminiscent of what occurs for the first and second sound in superfluid HeII: The second sound which corresponds to a temperature (and entropy) wave cannot be excited by oscillations of the container wall, contrarily to the usual density waves associated with the first sound; see, e.g., Ref. 36.

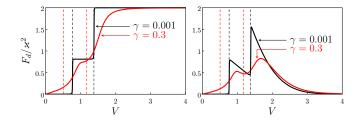


Figure 3. (Color online) Drag force  $F_d/\varkappa^2$  as a function of the velocity V of the obstacle relative to the condensate for two damping parameters:  $\gamma = 0.001$  (solid black curves) and  $\gamma = 0.3$  (solid red curves). The left plot corresponds to a point-like obstacle and the right plot to a Gaussian potential of width  $\ell = 0.5$ . The computation is done for  $\alpha = -0.2$  and  $\Omega = 0.5 \Omega_{\rm crit}$ . In this case  $V_{\rm crit}^{\rm (d)} = 0.76(2)$  and  $V_{\rm crit}^{\rm (p)} = 1.37(7)$ when  $\gamma = 0.001$ , whereas  $V_{\rm crit}^{\rm (d)} = 0.50(5)$  and  $V_{\rm crit}^{\rm (p)} = 1.17(3)$ when  $\gamma = 0.3$ . All these threshold velocities are indicated by vertical colored dashed lines in the figure.

Finally we emphasize that another effect of the existence of the spin degree of freedom is revealed in the absence of obstacle by the quantum fluctuations of the polarization. One can show that in a homogeneous con-

<sup>1</sup> J. Kasprzak *et al.*, Nature (London) **443**, 409 (2006).

- <sup>2</sup> R. Balili, V. Hartwell, D. Snoke, L. Pfeiffer, and K. West, Science **316**, 1007 (2007).
- <sup>3</sup> C. W. Lai *et al.*, Nature (London) **450**, 529 (2007).
- <sup>4</sup> S. Christopoulos *et al.*, Phys. Rev. Lett. **98**, 126405 (2007).
- <sup>5</sup> A. Amo *et al.*, Nature (London) **457**, 291 (2009).
- <sup>6</sup> A. Amo *et al.*, Nat. Phys. **5**, 805 (2009).
- <sup>7</sup> K. G. Lagoudakis *et al.*, Nat. Phys. **4**, 706 (2008).
- <sup>8</sup> G. Roumpos *et al.*, Nat. Phys. **7**, 129 (2011).
- <sup>9</sup> G. Nardin *et al.*, Nat. Phys. **7**, 635 (2011).
- <sup>10</sup> D. Sanvitto *et al.*, Nat. Phot. **5**, 610 (2011).
- <sup>11</sup> A. Amo *et al.*, Science **332**, 1167 (2011).
- <sup>12</sup> G. Grosso, G. Nardin, F. Morier-Genoud, Y. Léger, and B. Deveaud-Plédran, Phys. Rev. Lett. **107**, 245301 (2011).
- <sup>13</sup> I. Carusotto and C. Ciuti, Rev. Mod. Phys. **85**, 299 (2013).
- <sup>14</sup> L. V. Butov and A. V. Kavokin, Nat. Phot. 6, 2 (2012);
   B. Deveaud-Plédran, Nat. Phot. 6, 205 (2012).
- <sup>15</sup> C. Leyder *et al.*, Nat. Phys. **3**, 628 (2007).
- <sup>16</sup> K. G. Lagoudakis *et al.*, Science **326**, 974 (2009).
- <sup>17</sup> R. Hivet *et al.*, Nat. Phys. **8**, 724 (2012).
- <sup>18</sup> A. M. Kamchatnov, Y. V. Kartashov, P.-É. Larré and N. Pavloff, arXiv:1308.0784.
- <sup>19</sup> I. A. Shelykh, Y. G. Rubo, and A. V. Kavokin, Superlattice. Microst. **41**, 313 (2007).
- <sup>20</sup> Y. G. Rubo, A. V. Kavokin, and I. A. Shelykh, Phys. Lett. A **358**, 227 (2006).
- <sup>21</sup> D. Bajoni *et al.*, Phys. Rev. Lett. **100**, 047401 (2008).
- <sup>22</sup> S. Utsunomiya *et al.*, Nat. Phys. **4**, 700 (2008).
- <sup>23</sup> H. Flayac, H. Terças, D. D. Solnyshkov, and G. Malpuech, arXiv:1212.5894.
- <sup>24</sup> M. Wouters and I. Carusotto, Phys. Rev. Lett. **99**, 140402 (2007).
- <sup>25</sup> J. Keeling and N. G. Berloff, Phys. Rev. Lett. **100**, 250401

(2008).

- <sup>26</sup> M. Wouters, Phys. Rev. B **77**, 121302(R) (2008).
- <sup>27</sup> M. Wouters and I. Carusotto, Phys. Rev. Lett. **105**, 020602 (2010).

densate in the absence of damping and of magnetic field,

 $g_{\mathbf{p}}^{(2)}(x,x') = \langle :\delta \hat{\Pi}(x) \, \delta \hat{\Pi}(x') : \rangle$  is a universal function of

 $c_{\rm p}|x-x'|$  which goes to zero when  $|x-x'| \to \infty$ . One gets  $g_{\rm p}^{(2)}(x,x) = -\frac{2}{\pi}c_{\rm p} < 0$ : This corresponds to local sub-Poissonian fluctuations of the polarization. These fluctuations are strongly modified in the presence of a

(polarization) sonic horizon. They acquire nonlocal features associated to the correlated emission of analogous

Hawking radiation, as first shown in Refs. 37 for density-

density correlations. The present results suggest that in

polariton systems the polarization-polarization correla-

tion function  $g_{\rm p}^{(2)}(x,x')$  should be a quite efficient observable for witnessing Hawking radiation, even in the

ACKNOWLEDGMENTS

We thank A. Amo, J. Bloch and S. Stringari for

fruitful discussions. This work was supported by the French ANR under grant  $n^{\circ}$  ANR-11-IDEX-0003-02

absence of an external magnetic field<sup>38</sup>.

(Inter-Labex grant QEAGE).

- <sup>28</sup> M. O. Borgh, J. Keeling, and N. G. Berloff, Phys. Rev. B 81, 235302 (2010).
- <sup>29</sup> T. K. Paraïso, M. Wouters, Y. Léger, F. Morier-Genoud and B. Deveaud-Plédran, Nature Mater. 9, 655 (2010).
- <sup>30</sup> D. V. Fil and S. I. Shevchenko, Phys. Rev. A **72**, 013616 (2005).
- <sup>31</sup> L. Pitaevskii and S. Stringari, Bose-Einstein condensation (Clarendon Press, Oxford, 2003).
- <sup>32</sup> This is a standard value for the dimensionless parameter  $\gamma$  which is typically of order  $\hbar/(\tau\mu)$ ,  $\tau$  being the lifetime of a polariton ( $\tau \sim 10$  ps) and  $\mu$  the chemical potential ( $\mu \sim 0.5$  meV).
- <sup>33</sup> P.-É. Larré, N. Pavloff, and A. M. Kamchatnov, Phys. Rev. B 86, 165304 (2012).
- <sup>34</sup> This is not quite true because, as explained above, the distinction between density and polarization modes is not sharp.
- <sup>35</sup> A. Berceanu, E. Cancellieri, and F. M. Marchetti, J. Phys.: Condens. Matter 24, 235802 (2012).
- <sup>36</sup> L. D. Landau and E. M. Lifshitz, *Fluid Mechanics*, (Pergamon, 1959).
- <sup>37</sup> R. Balbinot, A. Fabbri, S. Fagnocchi, A. Recati, and I. Carusotto, Phys. Rev. A **78**, 021603 (2008); I. Carusotto, S. Fagnocchi, A. Recati, R. Balbinot, and A. Fabbri, New J. Phys. **10**, 103001 (2008).
- <sup>38</sup> P.-É. Larré and N. Pavloff, arXiv:1307.2843, to appear in EPL.